Influence of the short range nonlocal nucleon-nucleon interaction on the elastic *n-d* scattering: Below 30 MeV

P. Doleschall*
Research Institute for Particle and Nuclear Physics, P.O. Box 49, H-1525 Budapest, Hungary
(Received 6 October 2003; published 13 May 2004)

A previously defined short range nonlocal nucleon-nucleon (*NN*) interaction, which more closely matches common expectations and reproduces the ^{3}H and ^{3}He binding energies, is tested in elastic scattering. Nonlocal *P*-wave interactions with modified on-shell behavior were constructed in order to produce better low-energy *n-d* analyzing powers. At low energies some of the changes are due to the correct 3*N* binding energy, however, there are effects due to the characteristic properties of the nonlocal interactions. There is an indication that *p-d* calculations based on the present nonlocal *NN* interactions (with or without the modified *P*-wave interactions) would produce the same quality or better agreement with the low- and medium-energy experimental data than the corresponding local *NN* interaction plus 3*N* force model.

DOI: 10.1103/PhysRevC.69.054001 PACS number(s): 21.30.−x, 21.45.+v, 21.10.Dr, 25.40.Cm

I. INTRODUCTION

This paper is the continuation of an investigation reported earlier [1]. The INOY (inside nonlocal outside Yukawa tail) nonlocal interactions determined there have a shorter range than the earlier nonlocal interactions [2,3]. The local Yukawa tail was cut off in 1–3 fm region, i.e., below 1 fm there is no local potential at all while around 3 fm the local potential becomes the intact Yukawa tail. The internal nonlocal potential was subsequently fitted to the *NN* data with the local potential being kept fixed. The overlap region of the fixed local and the fitted nonlocal interactions is practically the same 1–3 fm interval as the cutoff region of the Yukawa tail, although the nonlocal interaction is rather small above 2–2.5 fm. Its bulk is within the 1.5 fm sphere, which satisfies a more rigorous expectation [5] for the range of the nonlocality.

The new shorter range $^1S_0$ INOY interactions [1] include already the charge independence and charge symmetry breaking (CSB) effects, i.e., the *nn*, *pp*, and *np* interactions are slightly different and fit properly the *pp* and *np* data, and the *nn* scattering length. The higher partial-wave components of the nonlocal interaction constructed in the present paper have no CSB effect: the nuclear parts of the *nn* and *pp* interactions are the same.

All interactions were calculated with equal neutron and proton masses and without electromagnetic terms, only nonrelativistic Coulomb interaction was taken into account for the *pp* pair with a charge distribution defined in Ref. [6]. The same approximation is applied for the Argonne v_{18} potential [7], however, a small correction to the nuclear part is added in order to reproduce the correct scattering lengths and deuteron binding energy. This modified Argonne potential (notated by ARGm) produces the same 3*N* binding energies [1] (within 1–2 keV accuracy) as the original Argonne one. Since the INOY interactions and the Argonne potentials (both the original and the modified ones) have the same long range tail, the modified Argonne potential (ARGm) could be used as a reference local potential to compare with the nonlocal INOY interactions.

The new IS (inside nonlocal outside Yukawa tail short range) nonlocal interactions [1] reproduce simultaneously the triton and ^{3}He binding energies with high precision, although this is a consequence of the low deuteron *D*-state probability (P_D=3.60%) and the proper tuning of the $^1S_0$ interactions. The IS $^1S_0$ and $^3SD_1$ interactions of Ref. [1] are phenomenological model *NN* interactions which do not seem to contradict the physical expectations about the nature of the *NN* interaction and reproduce the *NN* measurements with high precision.

The vector analyzing power puzzle is one of the oldest problems in the three-nucleon Faddeev calculations. Although it was evident that the low- and medium-energy vector analyzing powers strongly depend on the presence and on the on-shell behavior of the triplet *P*-wave interactions [8,9], the disagreement between the theory and experiments was partly due to the used simple rank-1 separable *NN* interactions. Later, improving the on-shell behavior of the separable $^3SD_1$ tensor force and decreasing the low-energy phase shifts of the $^3P_0$ interaction, a good description of the *p-d* nucleon analyzing power was achieved at 10 MeV [10], while the fit to the deuteron vector analyzing power was poorer. However, the comparison of the *n-d* calculations with the *p-d* measurements was problematic itself, and therefore no conclusion was made about the quality of the fits, especially that at energy 22.7 MeV the agreement between the experiments and calculations became worse. The first calculations with realistic *NN* potentials [11] showed the same problems of the vector analyzing powers. The newest *p-d* calculations by Kievsky *et al.* [12] did not produce better agreement with the experimental data in the 0–30 MeV region.

Earlier results [3] indicate that the disagreement between the calculated and measured vector analyzing powers is independent of the locality or nonlocality of the *NN* interaction. Since the low- and medium-energy vector analyzing powers are sensitive mostly to the on-shell behavior of the triplet *P*-wave interactions, modified (based on the allowed

*Email address: doles@rmki.kfki.hu

TABLE I. Parameters of the IS nn/pp and np interactions.

	$^1S_0(pp/nn)$	$^1S_0(np)$	$^3S_1$	$^3D_1$
V_l (MeV fm^{-3})	−408.0	−391.7	−255.9	0.0
a_l (fm^{-1})	2.6	2.519	2.463	
a'_l (fm^{-1})	1.650	2.0	2.0	
x_l (fm)	0.0	0.0	0.0	
x'_l (fm)	1.0	1.0	1.0	
V^i_{ll} (MeV fm^{-3})	1.839×10^4	1.217×10^4	6.672×10^3	3.811×10^3
	−237.966	−127.209	−198.713	−646.7
	−1.205	−0.7298	−0.4695	0.4105
$V^2_{ll}(nn)$ (MeV fm^{-3})	−244.755			
b^i_{ll} (fm^{-1})	1.950	1.737	1.592	0.7955
	1.8	1.210	1.151	1.392
	0.55	0.5	0.5	1.225
c^i_{ll} (fm^{-1})	1.6	1.7	1.761	0.3
	1.4	1.0	1.4	1.725
	0.55	0.5	0.6	1.5
z^i_{ll} (fm)	0.0	0.0	0.0	0.0
	0.42	0.45	0.45	0.7
	1.0	1.0	1.0	1.4

range of phase shifts defined by Tornow and Tornow [13]) triplet pp and np P-wave INOY interactions with shorter range were defined. Shorter range nonlocal $^1P_1$ and D-wave interactions (including the $^3DG_3$ state) fitted to the Nijmegen phase shifts [14] were also constructed. The nn interactions were chosen to be the nuclear part of the corresponding pp potentials. For higher partial-wave components of the NN interactions the modified Argonne v_{18} potential is used.

The low-energy N-d tensor analyzing powers in principle are suitable to extract the A_D/A_S ratio of the deuteron asymptotic normalization constants, although an actual analysis was not successful [15]. Other authors [16] reported a value of A_D/A_S=0.0256(4) extracted from tensor analyzing powers in sub-Coulomb (d,p) reactions, and at present this is the accepted value, although it is smaller than the value 0.0273(5) obtained from the $^2\mathrm{H}(d,p)^3\mathrm{H}$ reaction [15] or the

TABLE II. Parameters of the P- and F-wave interactions (the nonlocal part of the $^3P_0$ and $^3P_1$ interactions are identical for nn, pp, and np pairs).

	$^1P_1$	$^3P_0$	$^3P_1$	$^3P_2(pp/nn)$	$^3P_2(np)$	$^3F_2(pp/nn)$	$^3F_2(np)$
V_l (MeV fm^{-3})	−392.4	−440.0	−300.0	−150.0	−160.0	0.0	0.0
a_l (fm^{-1})	1.442	2.0	0.96	2.7	2.9		
a'_l (fm^{-1})	1.250	1.8	1.5	1.8	1.8		
x_l (fm)	0.0	0.0	0.0	0.0	0.0		
x'_l (fm)	1.0	1.0	1.0	1.0	1.0		
V^i_{ll} (MeV fm^{-3})	2.259×10^5	7.8×10^3	1.422×10^4	3.0×10^5	3.5×10^5	5.4×10^3	5.223×10^3
	382.0	−0.2	485.3	−224.2	−270.0	−26.38	−29.18
	−5.596		0.0183	−0.91	−0.87	−0.6314	−0.5482
b^i_{ll} (fm^{-1})	2.059	1.0	1.2	3.4	3.4	0.9516	0.9608
	0.7392	0.5	0.91	1.9	2.0	3.0	3.0
	0.7		0.3	0.62	0.62	0.6	0.6
c^i_{ll} (fm^{-1})	4.0	2.0	3.5	2.5	2.5	0.8	0.8
	2.3	1.0	2.0	1.0	1.0	1.2	1.2
	1.0		1.0	0.8	0.8	0.8	0.8
z^i_{ll} (fm)	0.0	0.0	0.0	0.0	0.0	0.0	0.0
	0.6	1.8	0.8	0.6	0.6	0.8	0.8
	1.2		1.6	1.2	1.2	1.2	1.2

TABLE III. Parameters of the D- and G-wave interactions.

	$^1D_2(pp/nn)$	$^1D_2(np)$	$^3D_2$	$^3D_3$	$^3G_3$
V_l (MeV fm^{-3})	−200.0	−200.0	−200.0	−148.2	0.0
a_l (fm^{-1})	2.0	2.0	2.0	2.228	
a_l' (fm^{-1})	1.6	1.6	1.6	1.5	
x_l (fm)	0.0	0.0	0.0	0.0	
x_l' (fm)	1.0	1.0	1.0	1.0	
V_{ll}^i (MeV fm^{-3})	1.150×10^5	8.0×10^4	1.55×10^5	1.06×10^5	3.0×10^3
	−173.0	−233.0	−68.4	100.4	−337.1
	−0.6660	−0.69	−0.8	−0.9393	−2.329
b_{ll}^i (fm^{-1})	1.8	1.65	1.9	1.926	0.6479
	1.4	1.5	0.845	3.0	0.8952
	0.55	0.55	0.6	0.6	0.6
c_{ll}^i (fm^{-1})	2.5	2.5	3.0	3.5	0.8
	1.5	1.5	1.5	1.5	1.2
	1.0	1.0	1.0	0.8	0.8
z_{ll}^i (fm)	0.0	0.0	0.0	0.0	0.0
	0.7	0.7	0.7	0.6	0.8
	1.4	1.4	1.4	1.2	1.2

value 0.0271(22) from a phase shift analysis of n-p scattering [17]. The local potentials produce deuteron D-state probability higher than 5–5.5% [18,19] and this leads to values for A_D/A_S around 0.0250–0.0255 [4]. Therefore the low A_D/A_S value is a necessity for the local potential picture, while the INOY interactions are capable of producing a lower deuteron D-state probability and a higher A_D/A_S value. Since the asymptotic normalization constants A_D/A_S of the

TABLE IV. Parameters of the tensor part of the nonlocal interactions ($l<l'$).

	$^3SD_1$	$^3PF_2(pp/nn)$	$^3PF_2(np)$	$^3DG_3$
V_t^1 (MeV fm^{-3})	−455.5	−46.14	−53.51	−749.5
a_l^1 (fm^{-1})	2.5	4.0	4.0	1.346
$a_{l'}^1$ (fm^{-1})	1.2	1.286	1.33	1.5
x_l^1 (fm)	0.0	0.0	0.0	0.0
$x_{l'}^1$ (fm)	0.9	1.0	1.0	1.0
V_t^2 (MeV fm^{-3})	23.86	−206.8	−186.7	−175.8
a_l^2 (fm^{-1})	1.158	1.973	1.894	1.076
$a_{l'}^2$ (fm^{-1})	2.0	1.435	1.444	1.5
x_l^2 (fm)	0.9	1.0	1.0	1.0
$x_{l'}^2$ (fm)	0.0	0.0	0.0	0.0
$V_{ll'}^i$ (MeV fm^{-3})	-5.227×10^3	5.835×10^3	4.781×10^3	1.004×10^4
	−12.53	34.48	34.10	226.4
	−0.08051	0.1748	0.1892	−0.3562
$b_{ll'}^i$ (fm^{-1})	1.843	3.0	3.0	3.0
	0.6554	1.3	1.329	1.602
	0.3204	0.6	0.6	0.6
$c_{ll'}^i$ (fm^{-1})	1.0	1.2	1.2	3.0
	0.3944	0.4	0.4	0.4
	0.6	0.8	0.8	0.8
$z_{ll'}^i$ (fm)	0.0	0.0	0.0	0.0
	0.6	0.85	0.85	0.85
	1.2	1.3	1.3	1.3

TABLE V. The singlet scattering lengths and effective ranges.

	ARG	CD-Bonn	ARGm	IS
a_{pp} (fm)	−7.8064	−7.8154	−7.8064	−7.8064
r_{pp} (fm)	2.788	2.773	2.784	2.769
a_{nn} (fm)	−18.487	−18.968	−18.487	−18.601
r_{nn} (fm)	2.840	2.819	2.839	2.824
a_{np} (fm)	−23.732	−23.738	−23.748	−23.748
r_{np} (fm)	2.697	2.671	2.696	2.678

TABLE VI. Deuteron properties, triplet scattering lengths, and effective ranges.

	ARG	CD-Bonn	ARGm	IS
ε_D (MeV)	−2.224575	−2.224575	−2.224575	−2.224582
P_D (%)	5.76	4.85	5.764	3.600
Q_D (fm^2)	0.270	0.270	0.2699	0.2751
A_S (fm$^{-1/2}$)	0.8846	0.8850	0.8851	0.8850
A_D/A_S	0.0250	0.0256	0.02509	0.02697
$r_{\rm rms}$ (fm)	1.967	1.966	1.96735	1.96514
a_t (fm)	5.419	5.4196	5.4192	5.4190
r_t (fm)	1.753	1.751	1.7532	1.7531

TABLE VII. The *pp* phase shifts (the unit of T_{lab} is MeV).

T_{lab}	$^1S_0$	$^3P_0$	$^3P_1$	$^3P_2$	ε_2	$^3F_2$
1	32.768	0.135	−0.087	0.014	−0.001	0.000
5	54.826	1.585	−0.975	0.213	−0.053	0.002
10	55.159	3.708	−2.244	0.651	−0.201	0.013
25	48.509	8.221	−5.406	2.522	−0.812	0.105
50	38.688	10.073	−8.981	6.000	−1.712	0.336
100	24.860	6.095	−13.769	11.411	−2.639	0.813
150	14.907	0.324	−17.717	14.587	−2.844	1.206
200	6.920	−5.128	−21.423	16.411	−2.746	1.447
250	0.108	−10.040	−24.983	17.434	−2.547	1.485
300	−5.911	−14.482	−28.416	17.896	−2.324	1.302
350	−11.335	−18.548	−31.714	17.912	−2.108	0.918

TABLE VIII. The *np* phase shifts (the unit of T_{lab} is MeV).

T_{lab}	$^1S_0$	$^3S_1$	ε_1	$^3D_1$	$^1P_1$	$^3P_0$	$^3P_1$	$^3P_2$	ε_2	$^3F_2$
1	62.078	147.740	0.114	−0.005	−0.188	0.179	−0.117	0.021	−0.001	0.000
5	63.620	118.168	0.734	−0.192	−1.493	1.623	−1.021	0.247	−0.049	0.002
10	59.939	102.604	1.270	−0.708	−3.053	3.627	−2.263	0.703	−0.183	0.011
25	50.870	80.641	1.924	−2.922	−6.332	7.814	−5.367	2.580	−0.754	0.089
50	40.522	62.839	2.126	−6.672	−9.659	9.438	−8.928	6.038	−1.627	0.298
100	26.811	43.398	2.337	−12.473	−14.449	5.405	−13.772	11.479	−2.558	0.740
150	16.941	30.871	2.761	−16.537	−18.618	−0.322	−17.783	14.781	−2.776	1.106
200	8.859	21.253	3.241	−19.574	−22.232	−5.729	−21.537	16.759	−2.685	1.330
250	1.832	13.293	3.697	−22.011	−25.214	−10.604	−25.132	17.922	−2.491	1.369
300	−4.459	6.446	4.120	−24.078	−27.609	−15.019	−28.585	18.496	−2.280	1.208
350	−10.176	0.424	4.518	−25.887	−29.551	−19.062	−31.899	18.591	−2.082	0.862

TABLE IX. The D- and G-wave phase shifts (the unit of T_{lab} is MeV).

T_{lab}	$^1D_2(pp)$	$^1D_2(np)$	$^3D_2$	$^3D_3$	ε_3	$^3G_3$
1	0.000	0.001	0.006	0.000	0.000	−0.000
5	0.043	0.041	0.222	0.002	0.013	−0.000
10	0.165	0.156	0.846	0.005	0.081	−0.004
25	0.696	0.682	3.710	0.045	0.553	−0.053
50	1.714	1.735	8.970	0.326	1.616	−0.262
100	3.790	3.905	17.251	1.494	3.504	−0.951
150	5.587	5.767	22.073	2.772	4.821	−1.758
200	7.060	7.284	24.481	3.731	5.699	−2.534
250	8.332	8.596	25.432	4.310	6.306	−3.236
300	9.488	9.793	25.506	4.584	6.771	−3.872
350	10.531	10.881	25.028	4.643	7.176	−4.470

deuteron produced by the IS and ISa [1] interactions are different, the dependence of the tensor analyzing powers, especially that of the T_{22}, on the value of A_D/A_S (or on the deuteron D-state probability) can be investigated.

The basic problem that n-d calculations are compared with p-d measurements is at least partially solved because a new set of p-d calculations was published [12], and the effect of the Coulomb interaction on the differential cross section and on the analyzing powers is given. Expecting a similar Coulomb effect for the nonlocal NN interactions, the n-d calculations could be compared with the p-d measure-

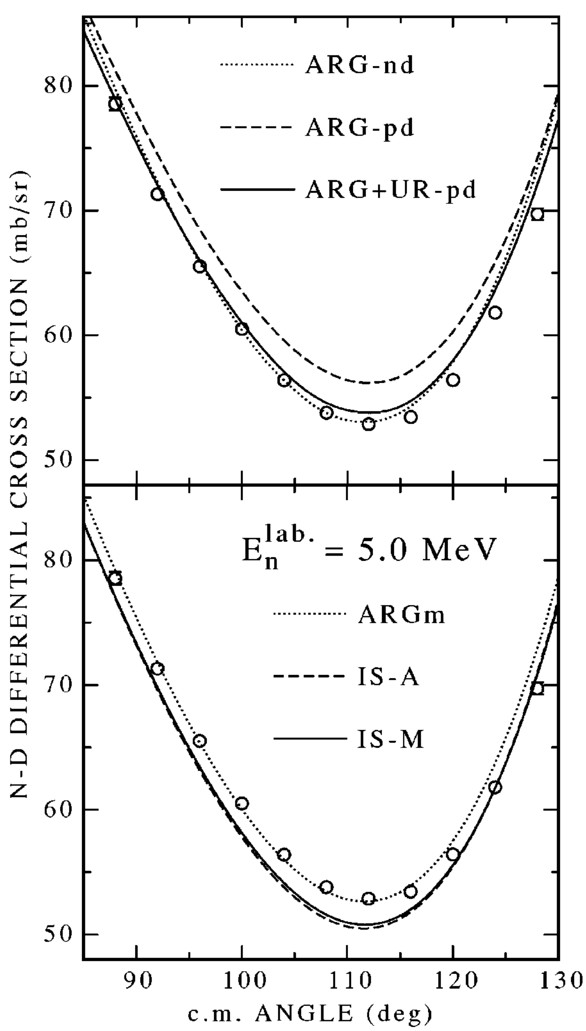

FIG. 1. Minimum of the N-d differential cross section. The experimental points are the p-d measurements of Sagara [12].

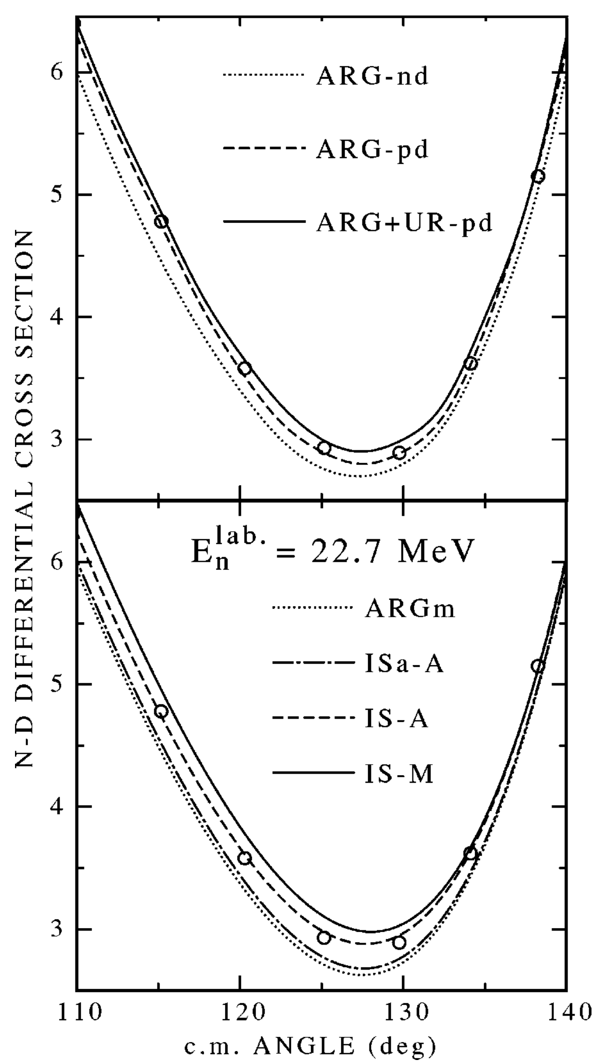

FIG. 2. Minimum of the N-d differential cross section. The experimental points are the p-d measurements of Ref. [32].

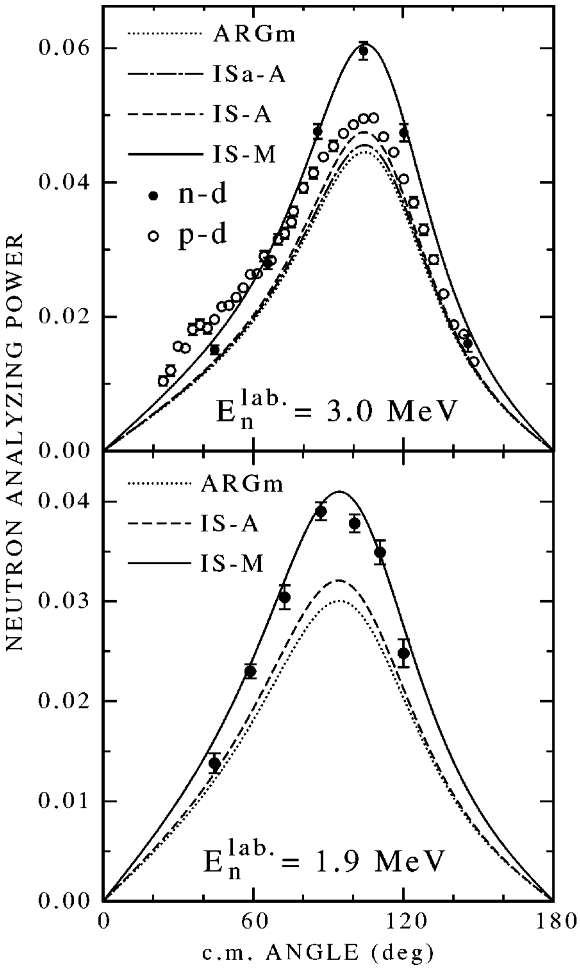

FIG. 3. Nucleon analyzing powers depending on the type of the *NN* interaction. The *n*-*d* experimental points at 3 MeV are from Ref. [25], at 1.88 MeV from Ref. [25], and the *p*-*d* experimental points are from Ref. [28].

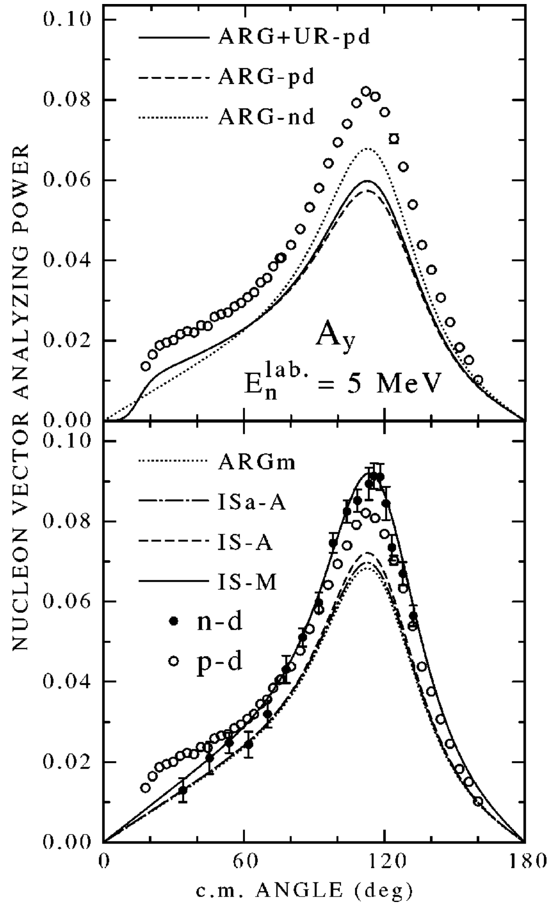

FIG. 4. Nucleon analyzing powers depending on the type of the *NN* interaction. The *n*-*d* experimental points are from Ref. [30] and the *p*-*d* experimental points are those of Sagara [12].

ments at least in a qualitative way. Of course *p*-*d* calculations with the INOY interactions would be necessary to give the accurate answer.

The properties of the constructed *P*- and *D*-wave INOY interactions are given in Sec. II. The effect of the INOY interactions on the elastic scattering is presented in Sec. III; the summary and conclusions are given in Sec. IV.

II. THE *P*- AND *D*-WAVE INOY *NN* INTERACTIONS

The shape of the INOY *NN* interaction is defined in Ref. [1]. Some parameters are fixed for all potentials. These are $\alpha_{ll'}=1.0$ fm^{-1}, $R_{ll'}=1.0$ fm, and $\beta_l=\gamma=2.0$ fm^{-1}. The number of diagonal terms ($n_{ll'}$) is equal to 3 except for the $^3P_0$ interaction for which $n_{ll'}=2$ is used.

The nuclear part of the *nn* and *pp* forces are identical for all INOY *P*- and *D*-wave interactions. It has to be emphasized also that within the presented framework the central parts of the INOY interactions already include the diagonal part of the tensor force in contrast to the usual formulation of local potentials. The parameters which are given with one or two digits are fixed ones, they were not fitted.

The *P*- and *D*-wave interactions were constructed with the same type off-diagonal attraction which was essential in cases of the INOY $^1S_0$ and $^3SD_1$ forces. As a consequence, the *P*- and *D*-state wave functions are also enhanced at short distance.

The $^1P_1$ and the *D*-wave interactions (including the $^3DG_3$ tensor force) fit the Nijmegen phase shifts [14] with high precision; the triplet *P*-wave interactions fit a slightly modified set of phase shifts which are nearly within the limits determined by Tornow and Tornow [13] for the *pp* *P*-wave phase shifts in the 10–100 MeV interval. The $^3P_0$ phase shifts were decreased, the $^3P_1$ phase shifts were increased in the absolute value (somewhat more than what was defined by Tornow and Tornow), and the $^3P_2$ phase shifts were increased relative to the corresponding Nijmegen phase shifts. The same magnitude of the change was applied for the *np* phase shifts, although the allowed ranges of change are larger [13]. In this way the $^3P_0$ interaction became less attractive, the $^3P_1$ interaction became more repulsive, and the $^3P_2$ is more attractive. It has to be emphasized that these modifications were achieved by the change of the nonlocal part of the interactions with an unaltered cutoff Yukawa tail, contrary to the modifications applied in Ref. [20], where the strength of triplet *P*-wave interactions were changed and consequently the Yukawa tail was also modified. The addi-

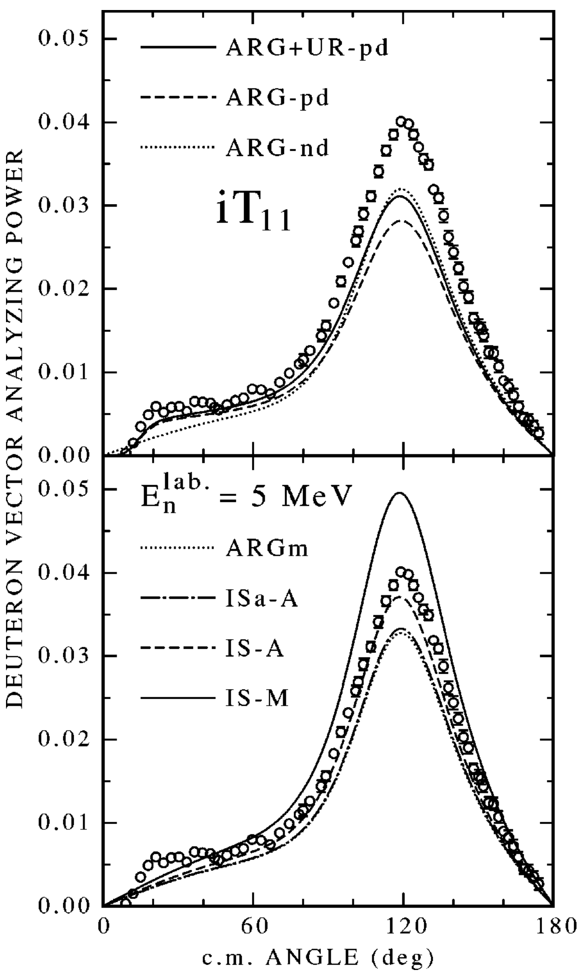

FIG. 5. Deuteron vector analyzing power depending on the *NN* interaction. The *p*-*d* experimental points are from Ref. [12].

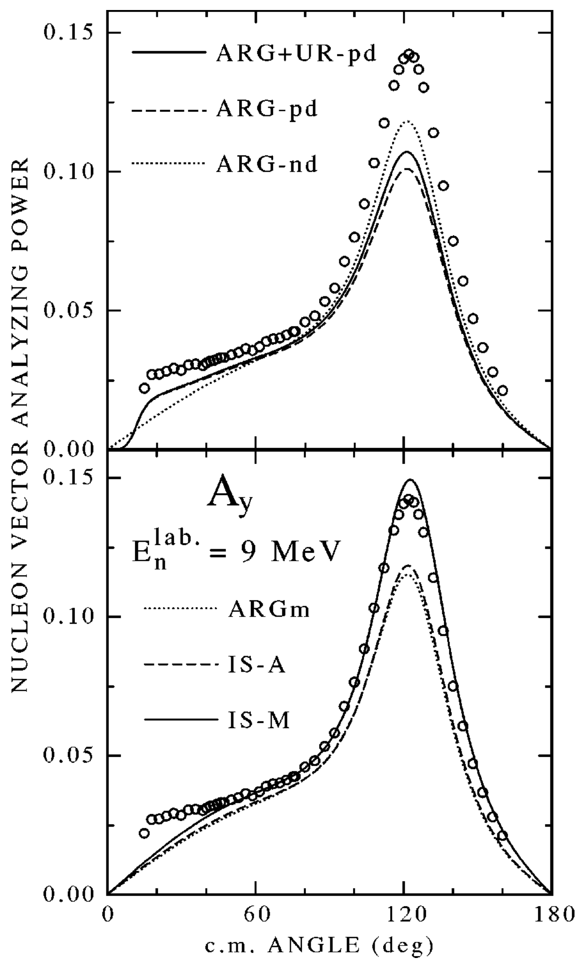

FIG. 6. Nucleon analyzing powers depending on the type of the *NN* interaction. The *p*-*d* experimental points are those of Sagara [12].

tionally chosen difference of the multipliers for the *nn* and *pp* pairs [20] is a strong CSB effect which is absolutely arbitrary, although not forbidden as a trial. In the present paper the nuclear parts of the *nn* and *pp* pairs are equal, which seems to be more realistic.

The parametrization of the short range INOY interactions are given in Tables I–IV, the singlet scattering lengths and effective ranges are shown in Table V, the deuteron properties, triplet scattering length, and effective range are shown in Table VI, and the phase shifts are shown in Tables VII–IX.

Because of the modified phase shifts of the triplet *P*-wave interactions, the new short range INOY *P*- and *D*-wave interactions are denoted as the set M interactions.

The set M of the *P*- and *D*-wave interactions were tuned to reproduce the ^{3}He binding energy with the IS set of $^1S_0$ and $^3SD_1$ interactions, however, ^{3}H became slightly under bound ($E_{\rm He}=-7.7181$ MeV, $E_{\rm H}=-8.4812$ MeV).

III. CALCULATIONS

Besides the above mentioned interactions the ISa tensor force [1], which reproduces the deuteron properties of the Argonne v_{18} [7] potential, was also used. The parametrization of this interaction is given in Ref. [1]. The *S*-state wave function of the ISa interaction is similar to those of the other INOY interactions: the internal part is enhanced as compared to the wave functions provided by the usual local potentials. It is the direct consequence of the chosen form of the nonlocality and it is also characteristic for the *S*-state wave functions of the Bonn potentials [21,22].

The higher partial-wave components of the *NN* interaction were cut off in the orbital angular momenta: up to an $l_{\rm max}$ value all components were taken into account and the coupling to the higher l values were neglected. At low and medium energies the $l_{\rm max}=3$ value proved to be sufficient, however, the $^3DG_3$ tensor force was included.

For Faddeev calculations separable expansions of the *NN* interactions were performed using the (Ernst-Shakin-Thaler) method [23]. The number of terms was varied and the satisfactory values are the following ones: rank-5 expansions for the $^1S_0$, $^1P_1$, $^3P_0$, $^3P_1$, $^1D_2$, and $^3D_2$, rank-4 expansions for the $^1F_3$, $^3F_3$, $^3F_4$, rank-11 expansion for the $^3SD_1$, and rank-10 expansion for the $^3PF_2$ and $^3DG_3$ interactions.

For the total angular momenta $J>11/2$ of the 3*N* system the solutions were substituted by a one term iteration of the Faddeev equation. The highest included total angular momentum was the $J=23/2$. The full Faddeev matrix for the $J\leqslant 11/2$ was also approximated: the coupling between the

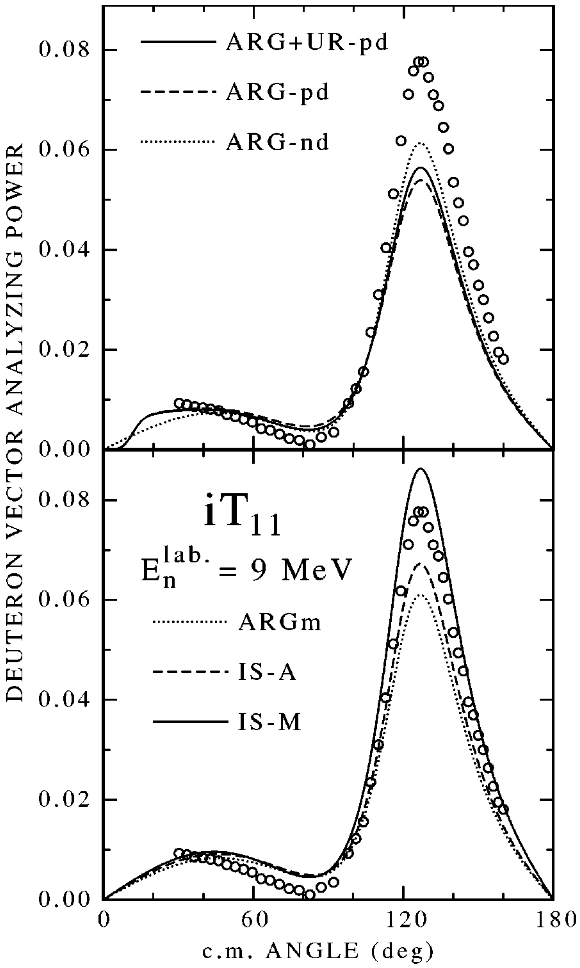

FIG. 7. Deuteron vector analyzing power depending on the *NN* interaction. The *p*-*d* experimental points are from Ref. [12].

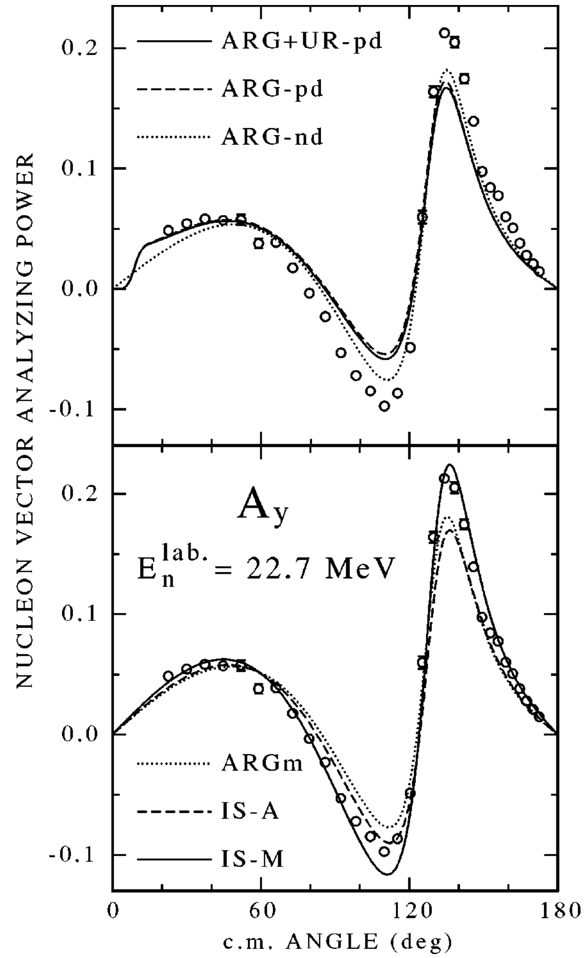

FIG. 8. Nucleon analyzing powers depending on the type of the *NN* interaction. The *p*-*d* experimental points are those of Sagara [32].

P-*F*, *D*-*F*, and *F*-*E* partial-wave components of the *NN* interactions were neglected [24]. All of these approximations were checked, and the accuracy is within the relative error of 1% for the measurable quantities.

The following notation is used in the figures.

(1) ARGm denotes that in all partial waves the modified Argonne v_{18} potential was used.

(2) ISa-A denotes that the $^1S_0$ interactions belongs to the set IS, the $^3SD_1$ interaction is the ISa one, and the rest is the Argonne potential.

(3) IS-A denotes that the $^1S_0$ and $^3SD_1$ interactions belong to the set IS and the rest is the Argonne potential.

(4) IS-M denotes that the $^1S_0$, $^3SD_1$, interactions belong to the set IS, the *P*- and *D*-wave interactions belong to the set M, and the rest is the Argonne potential.

(5) ARG-*nd* denotes the *n*-*d* calculations of the Kievsky *et al.* [12] with the original Argonne v_{18} interaction.

(6) ARG-*pd* denotes the *p*-*d* calculations of the Kievsky *et al.* [12] with the original Argonne v_{18} interaction.

(7) ARG+UR-*pd* denotes the *p*-*d* calculations of the Kievsky *et al.* [12] with the original Argonne v_{18} interaction plus an Urbana 3*N* force normalized to the 3*N* binding energy.

Calculations are made between nucleon laboratory energies 1–36 MeV. The *n*-*d* results are compared with Kievsky's [12] *n*-*d* and *p*-*d* results calculated with the original Argonne v_{18} interaction. The results are shown in Figs. 1–18.

A. The differential cross section

At low and medium energies some theoretical quantities depend on the 3*N* binding energy produced by the chosen *NN* (and a possible 3*N*) force. In the minimum of the differential cross section this scaling effect [29] is rather characteristic for the *n*-*d* scattering: below 12 MeV the increase of the triton binding energy deepens the minimum, above this energy the effect is the opposite. On the other hand, naturally, the scaling becomes weaker at higher energies: up to 9–10 MeV the difference in the minimum of the differential cross sections is caused by the different 3*N* binding energies, while at 22.7 MeV the scaling is responsible only for half of the effect.

The minimum of the differential cross section with the ARGm, ISa-A, IS-A, and IS-M sets at 5 MeV (Fig. 1) represents the scaling very characteristically (the set ISa-A produces practically the same result as the set ARGm). If the Coulomb shift of the minimum between the ARG-nd and

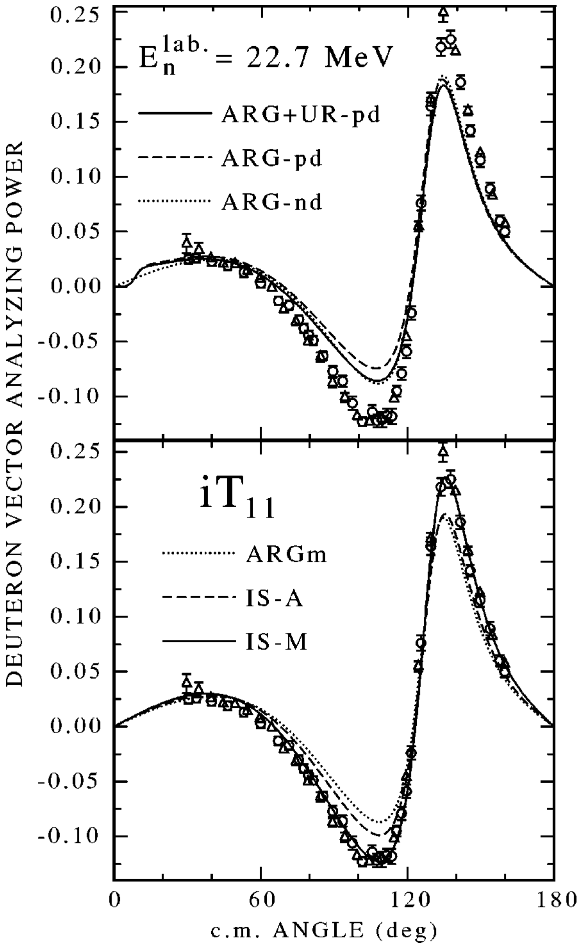

FIG. 9. Deuteron vector analyzing power depending on the *NN* interaction. The p-d experimental points are from Ref. [32].

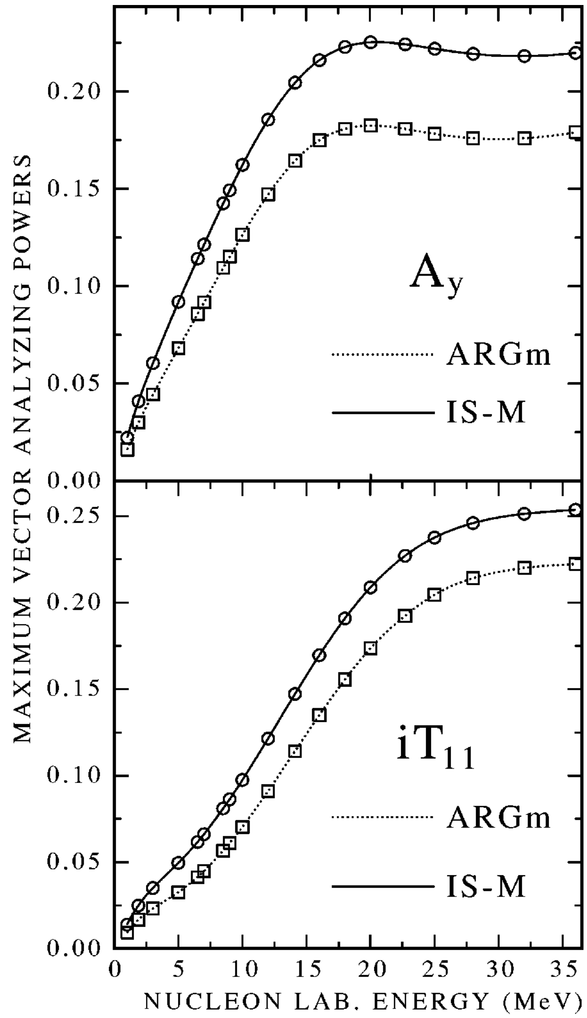

FIG. 10. Maximum of the calculated n-d vector analyzing powers depending on energy. The open circles and squares are the calculated values, and the curves are interpolations.

ARG-pd calculations is valid for n-d minimum of the IS-A and IS-M calculations, one gets a result near to the ARG+UR-*pd* one, which agrees rather well with the experimental values. However, the results at 22.7 MeV (Fig. 2) are less promising: the IS-A and IS-M results are already higher in the minimum than the p-d experimental data and the expected Coulomb shift [12] ought to push them even higher, while the ARG+UR-pd results are near to the experimental minimum. It has to be noted that the set ISa-A produces a slightly different result compared to the set ARGm, which could be a sign that at higher energies the different internal structure of the *NN* interactions has an effect.

B. The vector analyzing powers

The basic behavior of the nucleon and deuteron vector analyzing powers as a function of the *NN* interaction is rather similar. However, a more detailed comparison reveals some characteristic differences. The general feature is that the modified INOY *P*-wave interactions significantly improve the theoretical description of the vector analyzing powers (Figs. 3–9). It is shown again that the nonlocality itself has no significant influence on the vector analyzing powers: the results with the modified Argonne potential (ARGm) and with the set ISa-A (where the IS $^1S_0$ and the ISa $^3SD_1$ interactions substitute the corresponding Argonne potentials) are very near to each other. The effect by the IS-A interaction on the neutron analyzing power is mostly a scaling effect; on the deuteron vector analyzing power it is partly a scaling and partly an effect of the different deuteron *D*-state probability of the IS interaction.

Below the breakup threshold the neutron analyzing powers calculated with the IS-M set of interactions agree with the existing n-d measurements [25,26] (Fig. 3) and at nucleon laboratory energy 3 MeV the expected Coulomb shift [27] seems to produce a result near to the p-d measurement [28].

At nucleon laboratory energy 5 MeV (Figs. 4 and 5) the IS-M set of interactions seems to reproduce the experimental proton analyzing power if the Coulomb shift relative to the IS-M n-d result is the same as that of the Argonne potential. It has to be also noted that the IS-M result agrees with the existing n-d measurement [30]. However, the deuteron vector analyzing power of the set IS-M seems to have a maximum which is too high because the Coulomb shift seems not to be enough to decrease the n-d maximum to the p-d experimental values. Of course the accurate Coulomb effect for

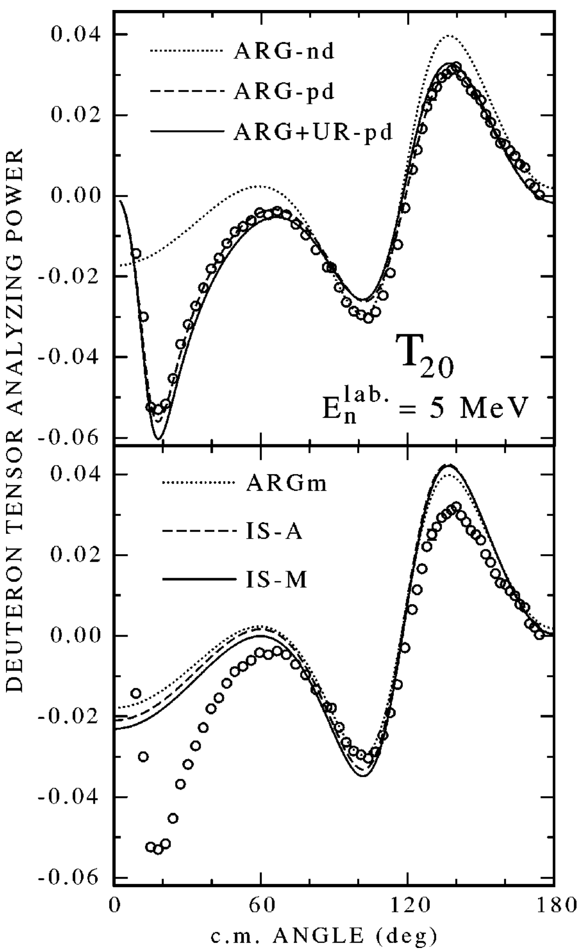

FIG. 11. Deuteron tensor analyzing power T_{20} depending on the *NN* interaction. The *p*-*d* experimental points are from Ref. [12].

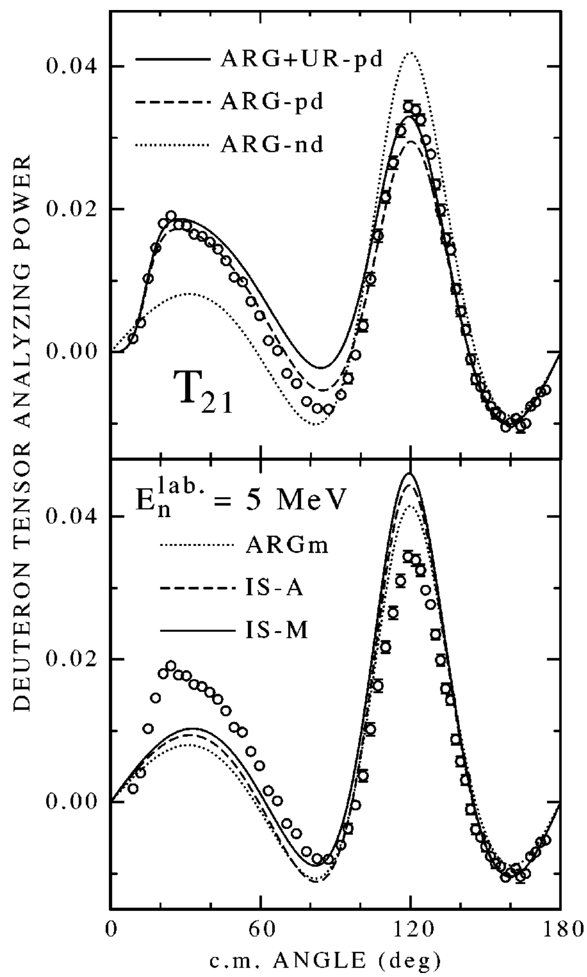

FIG. 12. Deuteron tensor analyzing power T_{21} depending on the *NN* interaction. The *p*-*d* experimental points are from Ref. [12].

the nonlocal interactions could be somewhat different.

At energy 9 MeV (and up to 14–16 MeV) the situation is the opposite: the Coulomb shift with the Argonne potential is too large to the IS-M *n*-*d* results (Fig. 6) to reproduce the maximum of the proton vector analyzing power, while the calculated deuteron vector analyzing power (Fig. 7) of the set IS-M seems to reproduce the *p*-*d* data if the Coulomb shift produced with the Argonne potential is valid.

At energy 22.7 MeV the minimum around the 110° c.m. (center of mass) angle becomes more characteristic than the maximum (Figs. 8 and 9) and both vector analyzing powers seem to become acceptable if the expected Coulomb shifts is applied to the *n*-*d* results of the IS-M set.

Finally the energy dependence of the maximum of the calculated *n*-*d* vector analyzing powers are plotted up to nucleon laboratory energy 36 MeV (Fig. 10). It can be seen that around 30–36 MeV the maximum seems to be stabilized which agrees with the higher-energy measurements.

C. The tensor analyzing powers

The deuteron tensor analyzing powers (Figs. 11–18) are basically determined by the $^3SD_1$ tensor force and modified by the *P*-wave interactions. This was known already in 1970s [31]. The nonlocality effect is very small (the ARGm and ISa-A results are nearly the same) and the modification of the *P*-wave interactions (IS-A versus IS-M) in most cases has a small or negligible effect. The largest difference is produced by the change of the $^3SD_1$ tensor force (IS versus ARGm).

The expected Coulomb effect seems to shift the *n*-*d* calculations with the set IS-M and IS-A to the proper direction. The only exception is the minimum of the T_{21} (Figs. 12 and 15). At energy 22.7 MeV the relative sensitivity to the different *NN* interactions becomes less, and all results seem to be satisfactory (Figs. 17 and 18), although the T_{22} with the IS interactions is better (Fig. 18) than the ARG+UR−*pd* result.

IV. SUMMARY AND CONCLUSIONS

The nonlocal interaction defined in Ref. [1] reproduces the 3*N* binding energies within a 1 keV accuracy without the introduction of a 3*N* force. The aim of the present work is the test of this interaction in the low- and medium-energy elastic scattering.

The basic conclusion is that the nonlocality itself has a very small effect on the low- and medium-energy scattering process. The results with the ISa-A set of interactions are

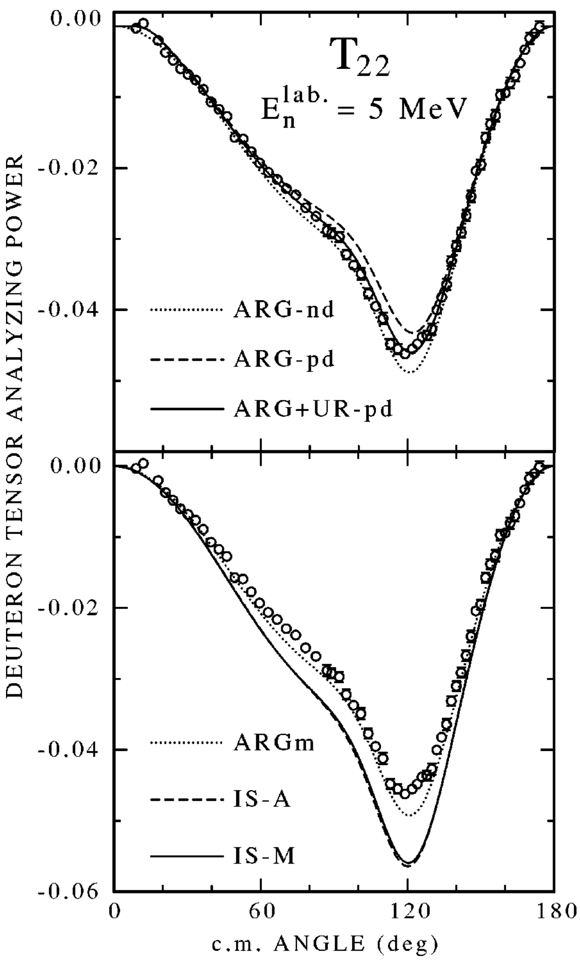

FIG. 13. Deuteron tensor analyzing power T_{22} depending on the *NN* interaction. The *p*-*d* experimental points are from Ref. [12].

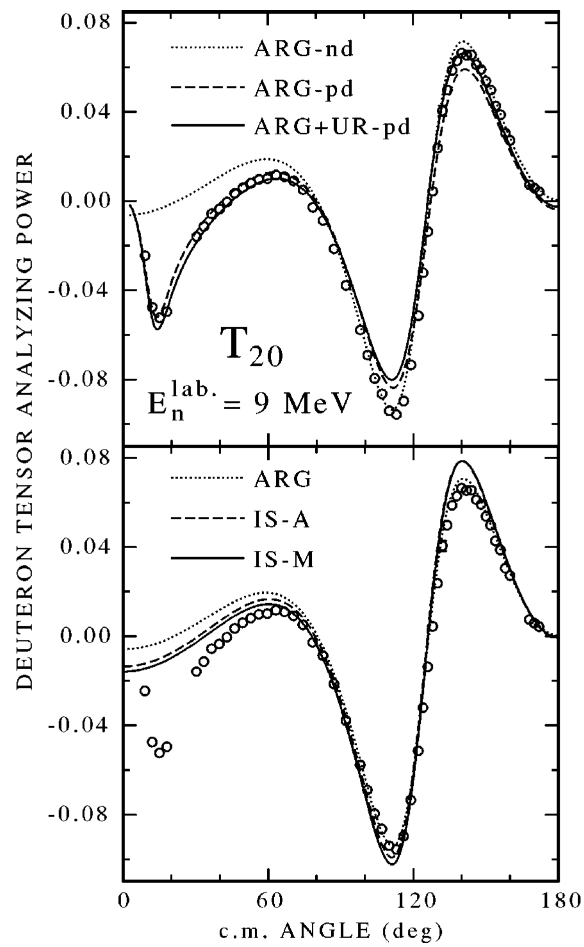

FIG. 14. Deuteron tensor analyzing power T_{20} depending on the *NN* interaction. The *p*-*d* experimental points are from Ref. [12].

practically the same as those with the modified Argonne potential (ARGm). Therefore it can be stated that a strong nonlocality of the *NN* interaction inside the 0–1.5 fm region and a weaker nonlocality (overlapping with the cutoff Yukawa tail) in the 1.5–3.0 fm region do not produce any significant deviation from the calculations with a local *NN* potential (in the present case the slightly modified Argonne potential) if the deuteron *D*-state probability and asymptotic normalization constant A_D/A_S are equal for both potentials. It has to be noted that the triton binding energies for the ISa-A set of interactions and for the ARGm potential are nearly the same [1], therefore even the scaling effect [29] is missing.

The situation is different if the nonlocal interaction produces different deuteron *D*-state probability and consequently different asymptotic normalization constant A_D/A_S. There are two effects caused by the IS-A set of interactions: one comes from the different triton binding energy (the scaling) and the second one comes from the different deuteron properties. The maximum of the neutron vector analyzing power produced by the IS-A set of interactions seems to exhibit the scaling effect: its change is proportional to the change of the minimum of the differential cross section (Figs. 3, 4, 6, and 8). However, the maximum of the deuteron vector analyzing power (Figs. 5, 7, and 9) does not follow this rule which is an indication that it additionally depends on the deuteron properties.

The IS-M set of interactions changes the vector analyzing powers due to the modification of the on-shell properties of the triplet *P*-wave interactions. It has also effects on other measurable quantities, however, these are less significant.

The scaling effect is characteristic for the minimum of the differential cross sections. Up to 10 MeV the scaling seems to be the dominant factor: if the 3*N* binding energy is correct, the minimum seems to agree with the experimental data independently whether the correct 3*N* binding energy is achieved with the local+3*N* force model or with the nonlocal INOY interactions. However, at higher energies the results are contradictory. At energy 22.7 MeV (Fig. 2) the best *p*-*d* minimum is produced by the Argonne interaction alone (ARG-*pd*). The INOY interactions (IS-A and IS-M) produce higher values for the minimum and there is an effect of the modified triplet *P*-wave interactions (IS-A versus IS-M). It is clear that if the expected Coulomb effect is the same as with the Argonne potential, the INOY interactions produce too high values for the minimum of the differential cross section. At energy 28 MeV, where the Coulomb effect is small, the local+3*N* force model gives too low minimum (1.9 mb/sr [12]), while the IS interaction is very near to the experimental minimum **(**2.19(2)mb/sr [34]**)**. However, the

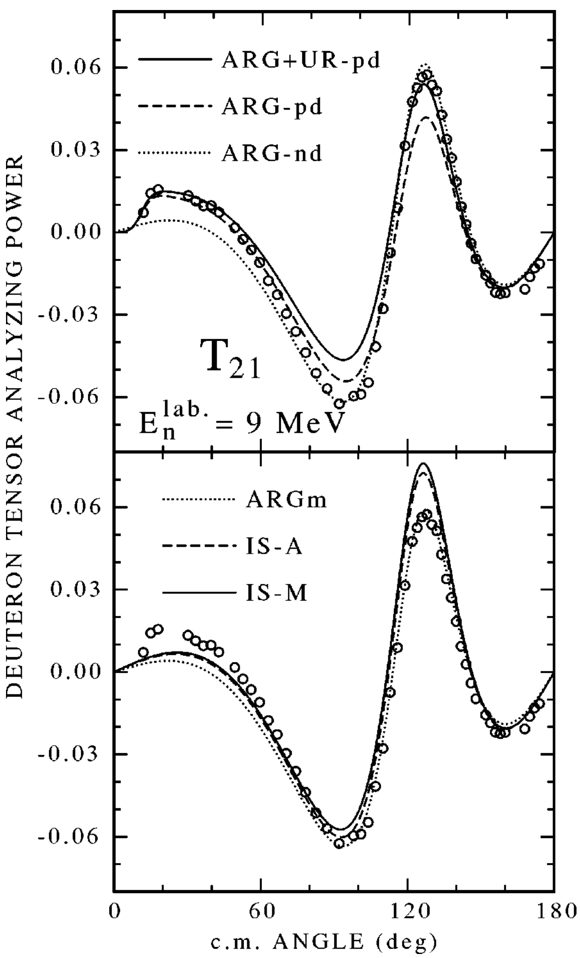

FIG. 15. Deuteron tensor analyzing power T_{21} depending on the *NN* interaction. The *p-d* experimental points are from Ref. [12].

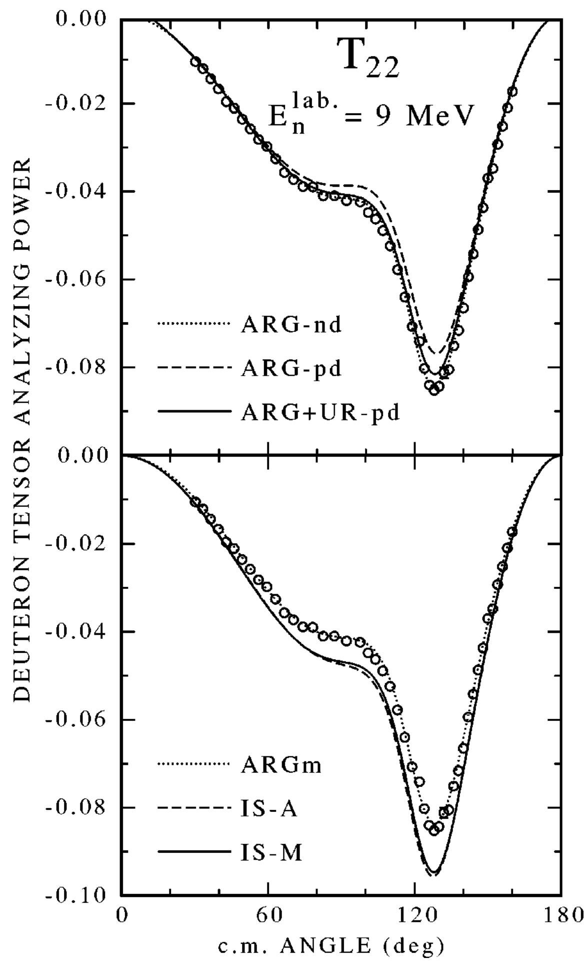

FIG. 16. Deuteron tensor analyzing power T_{22} depending on the *NN* interaction. The *p-d* experimental points are from Ref. [12].

backward experimental points at energy 28 MeV deviate from the calculations, while at energy 22.7 MeV they nearly coincide. This is a contradiction which may indicate that some of the measurements may be erroneous. There seems to be a problem.

It is evident that the experimental vector analyzing powers could not be reproduced without changing the on-shell behavior of the triplet *P*-wave interactions or without the introduction of a different 3*N* force [33]. The present choice of the modification of the triplet *P*-wave interactions is only a possibility which shows that with a very small change of the *pp* data fit [13], the *N-d* vector polarizations can be changed much more significantly. It has to be emphasized again that the rule of the modification is more rigorous than that of Witala and Glöckle [20]: (i) the Yukawa tail is unaltered and only the inside nonlocal part is changed; (ii) the nuclear parts of the *nn* and *pp* interactions are the same. The vector analyzing powers calculated with the IS-M set of interactions became significantly better, however, an improvement in the full 0–30 MeV energy interval was not achieved. There still seems to be a problem in the 5–15 MeV region, while below and above these energies both vector polarizations are described well by the present triplet *P*-wave interactions. Since the Coulomb effect is not necessarily exactly the same for the local and nonlocal interactions (see, for example, the different Coulomb shifts for the ^{3}He binding energy [1]), calculations with the Coulomb force have to be performed in order to find an answer to the problem of the energy dependence of the vector analyzing powers.

The tensor analyzing powers seem to be another case. Their sensitivity to the *P*-wave interactions (especially below 10–15 MeV) is much smaller than the effect caused by the different $^3SD_1$ forces. This effect is present already below the breakup threshold (at 2–3 MeV) and the T_{22} is the cleanest manifestation of the disagreement between the experiments and their theoretical description. At the low and medium energies the Coulomb effect cannot be neglected, and the beautiful description of the experimental *p-d* T_{22} around 10 MeV with *n-d* calculations using the Argonne v_{18} potential is misleading. The results of Ref. [12] clearly show that at energy 9 MeV (Fig. 16) the Coulomb effect is much above the experimental uncertainty at the backward angles, and this Coulomb effect removes the earlier agreement between the *n-d* calculations and *p-d* measurements. The calculation with the 3*N* force improves the result (this effect is mostly produced by the correct ^{3}He binding energy), however, at energy 22.7 MeV the effect of the 3*N* force is the opposite and moves the backward minimum of the theoretical T_{22} in the wrong direction (Fig. 18). Except for the energy 5 MeV (Fig.

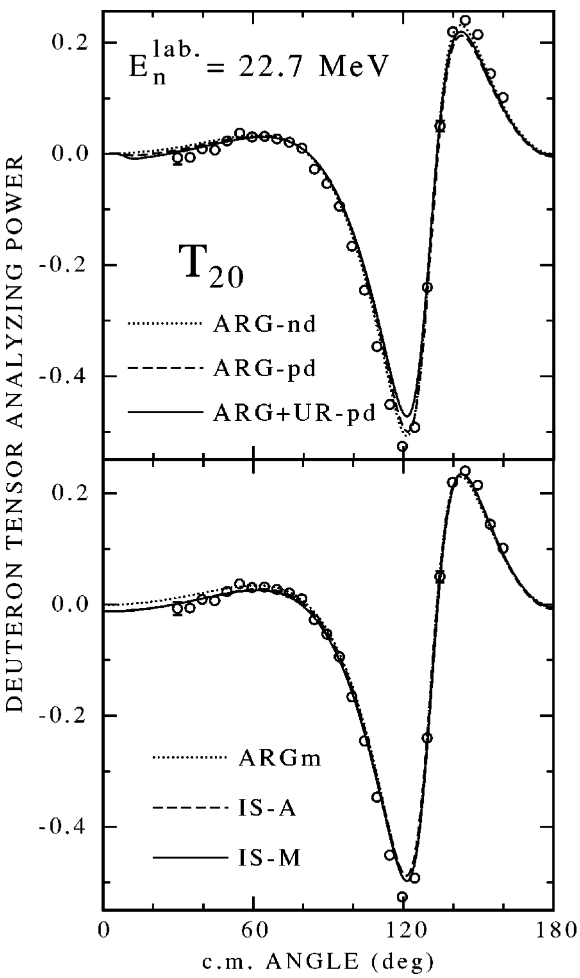

FIG. 17. Deuteron tensor analyzing power T_{20} depending on the *NN* interaction. The p-d experimental points are from Ref. [32].

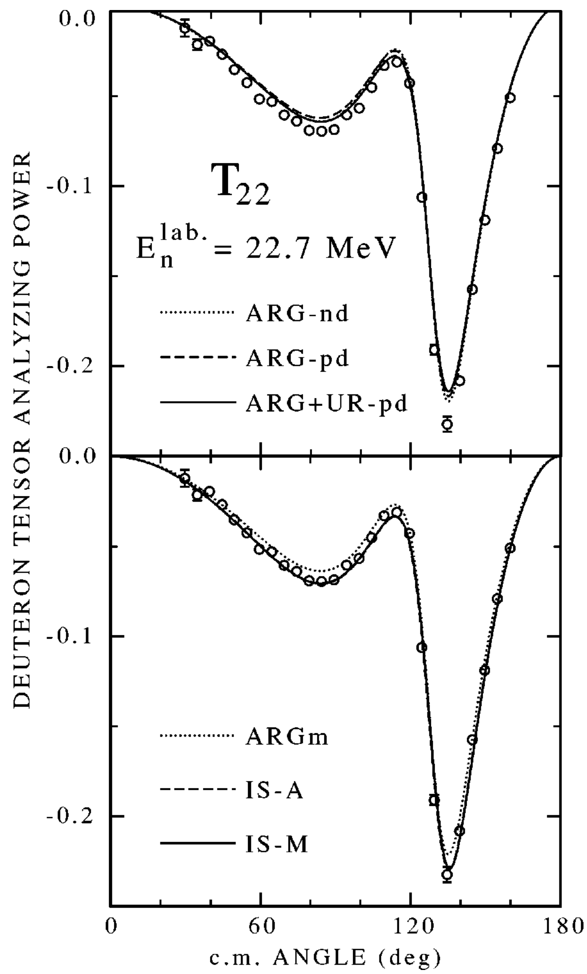

FIG. 18. Deuteron tensor analyzing power T_{22} depending on the *NN* interaction. The p-d experimental points are from Ref. [32].

13), where the measured minimum of T_{22} at c.m. angle 120° seems to be less than the expected p-d theoretical minimum, the theoretical values for the T_{22} with the IS interactions are better than those with the local+3*N* force model.

The T_{22} is singled out because it has a relatively simple structure, however, all tensor analyzing powers are sensitive to the new nonlocal IS tensor force. Part of this sensitivity is due to the scaling effect (the differences in 3*N* binding energies), and part is an effect of the different asymptotic normalization constant A_D/A_S. Unfortunately the scaling effect and that of the A_D/A_S cannot be separated since the 3*N* binding energies also depend on the deuteron *D*-state probability and consequently on the A_D/A_S [4]. However, the calculations with the 3*N* force normalized to the 3*N* binding energy deviates from the ones calculated with the IS interactions and the difference could be the effect of the different A_D/A_S value. Therefore the low-energy tensor analyzing powers may serve as a testing ground for the value of the asymptotic normalization constant A_D/A_S. In fact this feature of the tensor analyzing powers was used unsuccessfully in Ref. [15], but p-d calculations may perform the same job successfully.

The present results indicate that the low- and medium-energy tensor analyzing powers calculated with the INOY interactions may be capable of reproducing most of the tensor analyzing powers if the Coulomb shifts are similar to those with the local potential. The only exception is the minimum of the T_{21} around the 80°−90° at energy 5 and 9 MeV where both the IS interaction and the local+3*N* force models fail.

As a final result one may conclude that the nonlocal *NN* interactions do not produce any surprising effect for the low- and medium-energy elastic scattering and as a model nuclear force is comparable to the local+3*N* force model.

ACKNOWLEDGMENTS

The author thanks Dr. A. Kievsky for supplying their tabulated results and the unpublished experimental data of Sagara. The work has been supported by OTKA under Contract No. T034334.

[1] P. Doleschall, I. Borbély, Z. Papp, and W. Plessas, Phys. Rev. C **67**, 064005 (2003).
[2] P. Doleschall, Nucl. Phys. **A602**, 60 (1996); P. Doleschall and I. Borbély, Few-Body Syst. **27**, 1 (1999).
[3] P. Doleschall, Few-Body Syst. **23**, 149 (1998),
[4] P. Doleschall and I. Borbély, Phys. Rev. C **62**, 054004 (2000).
[5] J. Siemens and A. P. Vischer, Ann. Phys. (N.Y.) **238**, 167 (1995).
[6] N. Auerbach, J. Hüfner, A. K. Kerman, and C. M. Shakin, Rev. Mod. Phys. **44**, 48 (1972).
[7] R. B. Wiringa, V. G. J. Stoks, and R. Schiavilla, Phys. Rev. C **51**, 38 (1995).
[8] S. C. Pieper, Nucl. Phys. **A193**, 529 (1972); S. C. Pieper and K. L. Kowalski, Phys. Rev. C **5**, 306 (1972).
[9] P. Doleschall, Phys. Lett. **40B**, 443 (1972).
[10] P. Doleschall, W. Grüebler, V. König, P. A. Schmelzbach, F. Sperisen, and B. Jenny, Nucl. Phys. **A380**, 72 (1982).
[11] W. Plessas and J. Haidenbauer, Few-Body Syst., Suppl. **2**, 185 (1987); Y. Koike and J. Haidenbauer, Nucl. Phys. **A463**, 365c (1987); J. Haidenbauer, Y. Koike, W. Plassas, and H. Zankel, in *Proceedings of the International Workshop on Few-Body Approaches to Nuclear Reactions in Tandem and Cyclotron Energy Regions*, edited by S. Oryu and T. Sawada (World Scientific, Singapore, 1987); H. Witala, W. Glöckle, and T. Cornelius, Few-Body Syst., Suppl. **2**, 555 (1987); Nucl. Phys. **A491**, 157 (1989).
[12] A. Kievsky, M. Viviani, and S. Rosati, Phys. Rev. C **64**, 024002 (2001).
[13] T. Tornow and W. Tornow, Few-Body Syst. **26**, 1 (1999).
[14] V. G. J. Stoks, R. A. M. Klomp, M. C. M. Rentmeester, and J. J. Swart, Phys. Rev. C **48**, 792 (1993).
[15] I. Borbély, W. Grüebler, B. Vuaridel, and V. König, Nucl. Phys. **A503**, 349 (1989).
[16] N. L. Rodning and L. D. Knutson, Phys. Rev. C **41**, 898 (1990).
[17] G. J. Stoks, P. C. van Campen, W. Spit, and J. J. de Swart, Phys. Rev. Lett. **60**, 1932 (1988).
[18] B. F. Gibson, H. Kohlhoff, and H. V. Geramb, Phys. Rev. C **51**, R465 (1995).
[19] J. L. Forest, Phys. Rev. C **61**, 034007 (2000).
[20] H. Witala and W. Glöckle, Nucl. Phys. **A528**, 48 (1991).
[21] R. Machleidt, K. Holinde, and Ch. Elster, Phys. Rep. **149**, 1 (1987).
[22] R. Machleidt, Phys. Rev. C **63**, 024001 (2001); R. Machleidt, F. Sammarruca, and Y. Song, *ibid.* **53**, R1483 (1996).
[23] D. J. Ernst, C. M. Shakin, and R. M. Thaler, Phys. Rev. C **8**, 507 (1973).
[24] Gy. Bencze and P. Doleschall, Phys. Lett. **44B**, 235 (1973).
[25] J. E. McAninch, L. O. Lamm, and W. Haeberli, Phys. Rev. C **50**, 589 (1994).
[26] E. M. Neidel *et al.*, Phys. Lett. B **552**, 29 (2003).
[27] A. Kievsky, M. Viviani, and S. Rosati, Phys. Rev. C **52**, R15 (1995).
[28] K. Sagara, H. Oguri, S. Shimizu, K. Maeda, H. Nakamura, T. Nakashima, and S. Morinobu, Phys. Rev. C **50**, 576 (1994).
[29] T. Frederico, I. D. Goldman, and S. K. Adhikari, Phys. Rev. C **37**, 898 (1988).
[30] W. Tornow, C. R. Howell, M. Alohali, Z. P. Chen, P. D. Felsher, J. M. Hanly, R. L. Walter, G. Weisel, G. Mertens, I. Slaus, H. Witala, and W. Glöckle, Phys. Lett. B **257**, 273 (1991).
[31] P. Doleschall, Nucl. Phys. **A201**, 264 (1973).
[32] W. Grübler, V. König, P. A. Schmelzbach, F. Sperisen, B. Jenny, R. E. White, F. Seiler, and H. E. Roser, Nucl. Phys. **A398**, 445 (1983).
[33] A. Kievsky, Phys. Rev. C **60**, 034001 (1999).
[34] K. Hatanaka *et al.*, Nucl. Phys. **A426**, 77 (1984).